Molecular Characterization of the Follicle Defects in the Growth Differentiation Factor 9-Deficient Ovary

Julia A. Elvin, Changning Yan, Pei Wang, Katsuhiko Nishimori, and Martin M. Matzuk

Department of Pathology (J.A.E., C.Y., P.W., M.M.M.)
Department of Molecular and Human Genetics (J.A.E., M.M.M.), and
Department of Cell Biology (M.M.M.)
Baylor College of Medicine
Houston, Texas 77030

Department of Applied Biochemistry (K.N.)
Tohoku University
Sendai, Miyagi, Japan 981-8555

Growth differentiation factor-9 (GDF-9), a secreted member of the transforming growth factor-β superfamily, is expressed at high levels in the mammalian oocyte beginning at the type 3a primary follicle stage. We have previously demonstrated that GDF-9-deficient female mice are infertile because of an early block in folliculogenesis at the type 3b primary follicle stage. To address the molecular defects that result from the absence of GDF-9, we have analyzed the expression of several important ovarian marker genes. The major findings of our studies are as follows: 1) There are no detectable signals around GDF-9-deficient follicles for several theca cell layer markers [*i.e.* 17α-hydroxylase, LH receptor (LHR), and c-*kit*, the receptor for kit ligand]. This demonstrates that in the absence of GDF-9, the follicles are incompetent to emit a signal that recruits theca cell precursors to surround the follicle; 2) The primary follicles of GDF-9-deficient mice demonstrate an up-regulation of kit ligand and inhibin-α. This suggests that these two important secreted growth factors, expressed in the granulosa cells, may be directly regulated in a paracrine fashion by GDF-9. Up-regulation of kit ligand, via signaling through c-*kit* on the oocyte, may be directly involved in the increased size of GDF-9-deficient oocytes and the eventual demise of the oocyte; 3) After loss of the oocyte, the cells of the GDF-9-deficient follicles remain in a steroidogenic cluster that histologically resembles small corpora lutea. However, at the molecular level, these cells are positive for both luteal markers (*e.g.* LHR and P-450 side chain cleavage) and nonluteal markers (*e.g.* inhibin α and P-450 aromatase). This demonstrates that initially the presence of the oocyte prevents the expression of luteinized markers, but that the absence of GDF-9 at an early timepoint alters the differentiation program of the granulosa cells; and 4) As demonstrated by staining with either proliferating cell nuclear antigen (PCNA) or Ki-67 and TUNEL (terminal deoxynucleotidyl transferase-mediated dUTP nick end labeling) labeling, the granulosa cells of GDF-9-deficient type 3b primary follicles fail to proliferate but also fail to undergo cell death. This suggests that granulosa cells of type 3b follicles require GDF-9 for continued growth and also to become competent to undergo apoptosis, possibly through a differentiation event. Thus, these studies have enlightened us as to the paracrine roles of GDF-9 as well as the normal steps of granulosa cell and theca cell growth and differentiation within ovarian follicles. (Molecular Endocrinology 13: 1018–1034, 1999)

0888-8809/99/$3.00/0
Molecular Endocrinology

INTRODUCTION

The ovarian follicle is the functional unit of the female reproductive system, consisting of an oocyte surrounded by granulosa and theca cells. During normal folliculogenesis, oocyte growth and maturation are coordinated with granulosa and theca cell proliferation and differentiation within the follicular unit (reviewed in Ref. 1). Follicular recruitment of a quiescent primordial follicle into the growing pool is morphologically characterized by an increase in oocyte size and a squamous-to-cuboidal transition of the associated granulosa cells, followed by secretion of the glycoprotein-rich zona pellucida. Normally, once follicular growth is

initiated, the oocyte grows to full size, and the granulosa cells proliferate to form multiple layers of granulosa cells in response to intrafollicular signals (2). Preantral follicle development encompasses approximately seven doublings of the original granulosa cells and is regulated primarily by paracrine and autocrine mechanisms. In contrast, large follicles are responsive to both intraovarian and extraovarian regulation and actively participate in the hypothalamic-pituitary-gonadal axis. Unless rescued by elevated FSH, most multilayer preantral and early antral follicles undergo atresia, a degenerative process characterized by widespread apoptotic death of the granulosa cells. In surviving follicles, LH stimulates theca cell androgen production, while FSH stimulates granulosa cell proliferation, aromatization of androgens to estrogens, and LH receptor (LHR) expression (3). Follicular estrogen feeds back on both the hypothalamus and pituitary to trigger the LH surge, while granulosa cell-derived inhibin decreases pituitary FSH secretion. The ability of the mammalian ovary to produce and respond to this complex milieu of regulatory factors is essential for efficient reproductive function.

The mammalian transforming growth factor-β superfamily, the largest family of secreted proteins, consists of more than 30 members (4). *In vivo* studies have demonstrated that individual members of this family exhibit a wide range of key biological functions, including cellular differentiation during early development of the embryo (*e.g*. nodal, BMP-2, and BMP-4), development of the eye and kidney (*e.g.* BMP-7), craniofacial development [*e.g.* activin βA and transforming growth factor-β3 (TGF-β3)], suppression of the immune system (*e.g.* TGF-β1), and regulation of muscle mass [*e.g.* growth differentiation factor-8 (GDF-8)] (5). Members of this family have also been shown to play essential roles during mammalian sexual differentiation and in gonadal function (5, 6). For example, absence of Müllerian inhibiting substance results in male pseudohermaphroditism, absence of inhibin-α leads to ovarian and testicular tumors, and absence of BMP-8a and BMP-8b, important testicular proteins, results in male infertility due to defects in spermatogenesis. GDF-9, BMP-15, and BMP-6 are TGF-β superfamily members expressed in the mammalian oocyte beginning at the type 3a follicle (one-layer) stage and expressed through ovulation (4, 7, 8). Using the GDF-9 knockout mice (9), we have previously shown that absence of GDF-9 results in a block in folliculogenesis at the type 3b stage (late, one-layer primary follicle stage). In addition, we have demonstrated that there are other secondary effects of absence of GDF-9, including apparent failure of the thecal layer to form and defects in the oocyte (9, 10). Among the changes that occur in the oocyte are defects in oocyte meiotic competence, including abnormal germinal vesicle breakdown and spontaneous parthenogenetic activation, and an increased rate of growth of the oocyte. In the present study, we have examined the molecular changes within the ovary that result from the absence of GDF-9. Our findings are important in defining the key role of GDF-9 in follicle development as well as contibuting to the understanding of normal ovarian physiology.

RESULTS

Cell Cycle Progression

GDF-9-deficient follicles with intact oocytes contain only one layer of granulosa cells and fail to form follicles consisting of multiple layers of granulosa cells. We hypothesized that this lack of increase in granulosa cell number is due to either a lack of granulosa cell proliferation or to an increase in granulosa cell apoptosis. Proliferating cell nuclear antigen (PCNA), a cofactor of DNA polymerase δ and cyclin-cdk complexes, is expressed during G_1, increases through the G_1/S transition, is high in G_2, and declines sharply in M phases of the cell cycle (11). Similarly, Ki-67, a component of the granular nucleolus, is expressed in all cell cycle phases except G_0 (12). The most highly proliferative granulosa cells are found in the wild-type antral follicle, in which the majority of the granulosa cells are PCNA (Fig. 1A) and Ki-67 positive (data not shown). In type 3b (large one-layer) and type 4 (two-layer) follicles of wild-type ovaries, immunohistochemical analysis of PCNA (Fig. 1, B and C) or Ki-67 (data not shown) showed that more than 50% of the granulosa cells in the cross-sections are positive (*i.e.* positive defined as intense red staining of the nucleus; negative defined as light or diffuse staining of the nucleus and cytoplasm). In contrast, the type 3b follicles with intact oocytes in the GDF-9-deficient ovary demonstrated less than 10% positive staining granulosa cells per cross-section (Fig. 1E), suggesting that nearly all of the granulosa cells are blocked at G_0. However, soon after oocyte degeneration, granulosa cell differentiation begins to occur in the follicles of the GDF-9-deficient ovary, and more cell nuclei stain positively for both PCNA (Fig. 1, D–F) and Ki-67 (data not shown). Oocyte nuclear staining with the PCNA antibody is detected in growing and full-grown oocytes of GDF-9-deficient type 3a and 3b follicles, consistent with previous studies demonstrating the presence of PCNA in nuclei of oocytes of primary through antral follicles in wild-type ovaries (11).

TUNEL (Terminal Deoxynucleotidyl Transferase-Mediated dUTP Nick End Labeling) Labeling

Although normal follicular development in the GDF-9-deficient ovaries arrests at the type 3b stage and oocyte loss eventually results in granulosa cell differentiation, histological examination of the GDF-9-deficient ovaries surprisingly failed to detect any apoptotic-appearing cells. To confirm the relative absence of apoptotic cells in the GDF-9-deficient ovaries, we

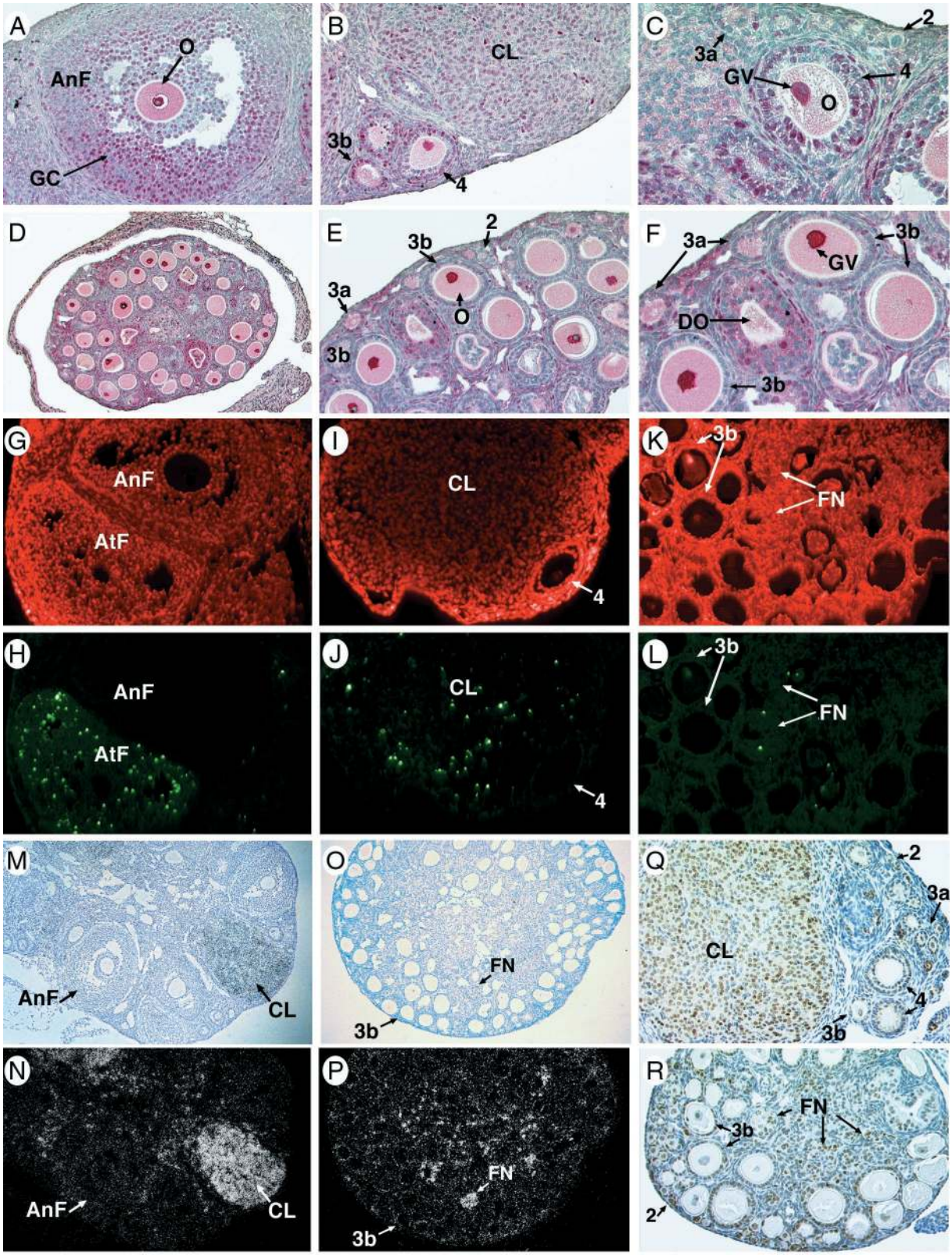

Fig. 1. Immunohistochemical and *in Situ* Hybridization Analysis of Ovarian Cell Cycle Markers

A–F, Ovaries from 9-week-old control (A–C) and GDF-9-deficient (D–F) mice were stained with an anti-PCNA monoclonal antibody. A, A large antral follicle (AnF) with positively staining (*dark red*) granulosa cells (GC) and cumulus cells (CC) (low power). B and C, One-layer (type 3b) and two-layer (type 4) follicles contain multiple positive nuclei and positive germinal vesicle (GV). The adjacent corpus lutea (CL) contains a few elongated, darkly staining cells (true positive) as well as diffusely staining luteinized

used a TUNEL assay to fluorescently label DNA ends. Granulosa cells of wild-type atretic antral follicles and corpora lutea contained many positively labeled cells (Fig. 1, G–J). In contrast, sections of GDF-9-deficient ovaries contained 2–10 positively labeled cells per ovarian section (Fig. 1, K and L). No positively staining cells were found in the one-layer follicles, but an occasional apoptotic cell was seen in follicles with degenerating oocytes, within the steroidogenic follicular nests, or within the interstitial tissue. Thus, in the absence of GDF-9, the majority of granulosa cells of the type 3b follicle appear to remain dormant and fail to either proliferate or die.

Analysis of Cell Cycle Inhibitors

p21 and p27 are well documented inhibitors of the cell cycle and are correlated with cell cycle arrest upon luteinization in the ovary (13). Based on the relative lack of proliferation of the granulosa cells in the GDF-9 knockout ovaries, we examined expression of both p21 and p27 mRNA by *in situ* hybridization and p27 protein by immunohistochemistry. p21 mRNA was detected at low levels ubiquitously in both wild-type and GDF-9-deficient ovaries with higher levels in wild-type atretic follicles and scattered cells in the corpora lutea, and in the luteinized follicular nests of the GDF-9-deficient ovary (data not shown). In wild-type ovaries, p27 mRNA is also expressed ubiquitously at low levels throughout the ovary but is more abundant in the corpora lutea of wild-type ovaries (Fig. 1, M and N). In the GDF-9-deficient ovary, granulosa cells of the one-layer follicles express detectable levels of p27 message, while small groups of cells in the center of the GDF-9-deficient ovary express higher levels (Fig. 1, O and P). Similarly, nuclear p27 immunoreactivity is clearly detectable in the majority of luteinized granulosa cells within the wild-type corpus luteum (Fig. 1Q), and within the luteinized follicular nests of the GDF-9-deficient ovary (Fig. 1R). Reduced p27 nuclear staining is also present in granulosa cells of both wild-type and GDF-9-deficient one-layer follicles, which is clearly higher than the staining in the negative control or in the interstitial cells (Fig. 1, Q and R). Although it is impossible to estimate protein levels by immunohistochemistry, there does not appear to be a dramatic difference in p27 immunoreactivity between the one-layer follicles of the GDF-9 knockout and wild-type ovaries. This suggests that p27 protein overexpression is not the reason for the block in folliculogenesis at the primary follicle stage in the GDF-9-deficient ovaries.

Thecal Layer Development

We have previously reported that a morphologically distinct thecal layer could not be detected by light and electron microscopic analysis in GDF-9-deficient ovaries (9). However, a flattened layer of fibroblastic cells outside of the granulosa cell basement membrane rings the type-3b follicles in the GDF-9-deficient ovaries. To confirm the absence of a true thecal layer, *in situ* hybridization was carried out with a probe for cytochrome P-450 17α-hydroxylase (17α-OH), a theca cell-specific enzyme necessary for androgen production. In the wild-type ovary, cells expressing 17α-OH begin to associate with type 3b and type 4 follicles and form complete rings just outside the granulosa cell basement membranes by the multilayer preantral follicle stage (Fig. 2, A and B). In contrast, in the GDF-9-deficient ovaries, only a few cells expressing 17α-OH are scattered in the interstitium and not associated with follicles (Fig. 2, C and D). These 17α-OH-positive cells may represent a theca cell precursor population that is responding to the elevated serum LH (9). Similarly, absence of LHR and c-*kit* mRNA around the follicle (see below) confirms that a theca cell layer fails to form. These data suggest that GDF-9 signaling is required either directly or indirectly to re-

granulosa cells (nonproliferating) (B, low power; C, high power). In panel C a cluster of small follicles in the wild-type ovary contains a high proportion of positively staining nuclei in a type 4 follicle, a single stained nuclei in the type 3b follicle, and no staining of the primordial (type 2) follicle. D, Low power (D) and high power (E and F) views of a GDF-9-deficient ovary demonstrates normal and abnormal follicles including oocyte-containing one-layer follicles (type 2, 3a, and 3b), which occupy the periphery, and follicles with degenerating oocytes (DO) and follicular nests, which predominate in the center of the section. In panels E and F, large type 3b follicles have few PCNA-positive granulosa cells, but oocytes (O) demonstrate intense PCNA-positive staining of the GV. Type 3a follicles and follicles with degenerating oocytes (DO) have multiple positive granulosa cells. G–L, Apoptosis detection in control (G–J) and GDF-9-deficient (K and L) follicles. All nuclei stained with propidium iodide (*red*), and apoptotic nuclei were labeled *green* by modified TUNEL with fluorescein detection (low power). G and H, A healthy antral follicle (AnF) and an atretic follicle (AtF) showing apoptotic nuclei in the atretic follicle in panel H. I and J, Scattered apoptotic nuclei in a corpus luteum are also seen in panel J but are absent in an adjacent healthy type 4 follicle. K and L, Several apoptotic nuclei are present in the follicular nests (FN) as seen in panel L, but elsewhere the apoptotic cells are absent. M–R, p27 expression in control (M, N, and Q) and GDF-9-deficient (O, P, and R) ovaries. M–P, p27 mRNA expression was analyzed by *in situ* hybridization using a specific cDNA antisense probe. Hybridization signal is visualized by darkfield illumination (N and P), and can be compared with tissue morphology in brightfield panel (M and O, low power). Q and R, p27 protein is detected by immunohistochemistry (*brown*), and nuclei are counterstained with hematoxylin (*blue*). In control ovaries, p27 is expressed at high levels in most cells of the corpus luteum (CL) and primordial follicles (type 2) and at low levels in preantral follicles (*e.g.* type 3a, 3b, and 4). In GDF-9-deficient ovaries, high levels are detected in some cells of the luteinized follicular nests (FN) and primordial follicles (type 2), while lower levels are seen in granulosa cells of type 3b follicles.

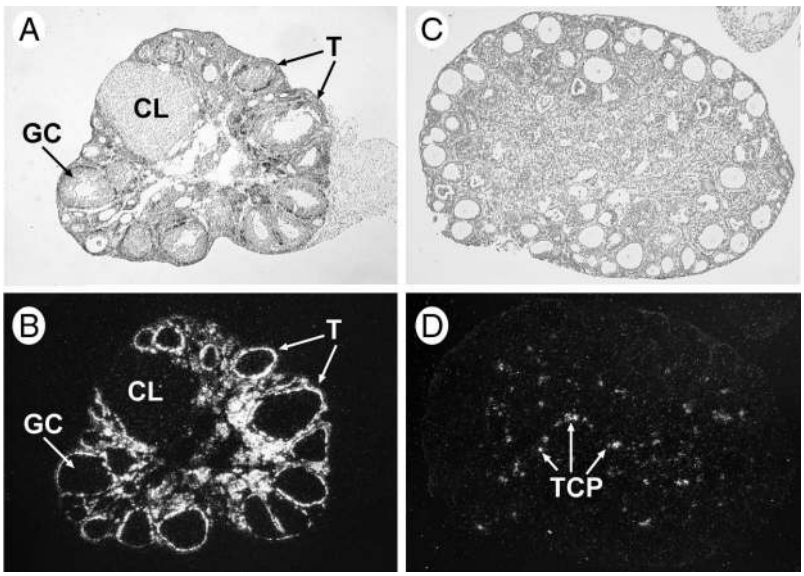

Fig. 2. Localization of 17α-Hydroxylase mRNA

Expression of 17α-hydroxylase mRNA in adult control (A and B) and GDF-9-deficient (C and D) ovaries was analyzed by *in situ* hybridization using specific cDNA antisense probes. Control ovaries show 17α-OH-expression in theca cells (T) while granulosa cells (GC) and cells of the corpora lutea (CL) are negative (low power). C and D, A few scattered 17α-OH-positive cells in the GDF-9-deficient ovary represent theca cell precursors (TCP), which do not ring follicles to form a theca layer (intermediate power).

cruit theca cell precursors to the early preantral follicles.

Analysis of c-*kit* and kit Ligand Expression

The c-*kit*/kit ligand-signaling pathway has been shown to be important for germ cell proliferation and folliculogenesis (14–16). By Northern blot analysis, we show that c-*kit* mRNA is expressed in GDF-9-deficient ovaries and that levels are comparable to or slightly higher than wild-type ovaries (Fig. 3B). By *in situ* hybridization, c-*kit* mRNA is localized to the oocyte and theca-interstitial cells of the wild-type ovary, but is excluded from granulosa cells as previously demonstrated (Fig. 4, A and B and Ref. 17). In the GDF-9-deficient ovaries, c-*kit* mRNA localizes only to oocytes, with only background levels of silver grains present over other cell types (Fig. 4, C–F).

In contrast to the c-*kit* expression results, kit ligand (KL) expression in GDF-9-deficient ovaries is increased 32-fold compared with expression in wild-type ovaries (Fig. 3B). Insulin-like growth factor-I (IGF-I), which is also expressed in the granulosa cells of early preantral follicles, however, does not show a similar increase in expression in the GDF-9-deficient ovary (Fig. 3D), suggesting that the increase in kit ligand represents a specific regulatory interaction, rather than a tissue composition effect. Although *in situ* hybridization is not a reliable method for quantitating mRNA expression, we can compare relative expression levels between wild-type and GDF-9-deficient ovaries by positioning sections from both types of ovaries close together on the same slide to minimize interslide variability. Under these conditions, we can barely detect kit ligand expression in the wild-type ovary (Fig. 4, G and H), with a faint signal above background apparent in granulosa cells of preantral follicles. In contrast, in the GDF-9-deficient ovaries, granulosa cell expression of kit ligand is abundant (Fig. 4, I and J). Type 3a and early type 3b follicles have detectable levels of kit ligand, while the largest one-layered follicles show more intense staining (Fig. 4, K and L). In the event that paracrine factors produced by multilayered follicles of adult ovaries repressed kit ligand expression, we examined ovaries from 10-, 17-, and 28-day-old wild-type mice. Although kit ligand was somewhat easier to detect in these immature ovaries because of the increased number of preantral follicles, the relative expression level per follicle was never comparable to the level seen in the GDF-9-deficient ovaries at similar ages (data not shown). Kit ligand expression is increased further in the granulosa cells of asymmetric follicles, which are presumably destined to undergo oocyte degeneration (Fig. 4, K and L). However, soon after the oocyte degenerates, kit ligand expression disappears (Fig. 4, I and J) and is also absent in the follicular nests.

There are two alternatively-spliced forms of kit ligand, KL-1 and KL-2, which differ by 84 bp. This alternative splicing results in an additional 28 amino acids in KL-1, which includes a proteolytic cleavage site. Since membrane-bound kit ligand is more active than free kit ligand, KL-2, the more stable, cell-associated form, is consequently more potent (14). By non-

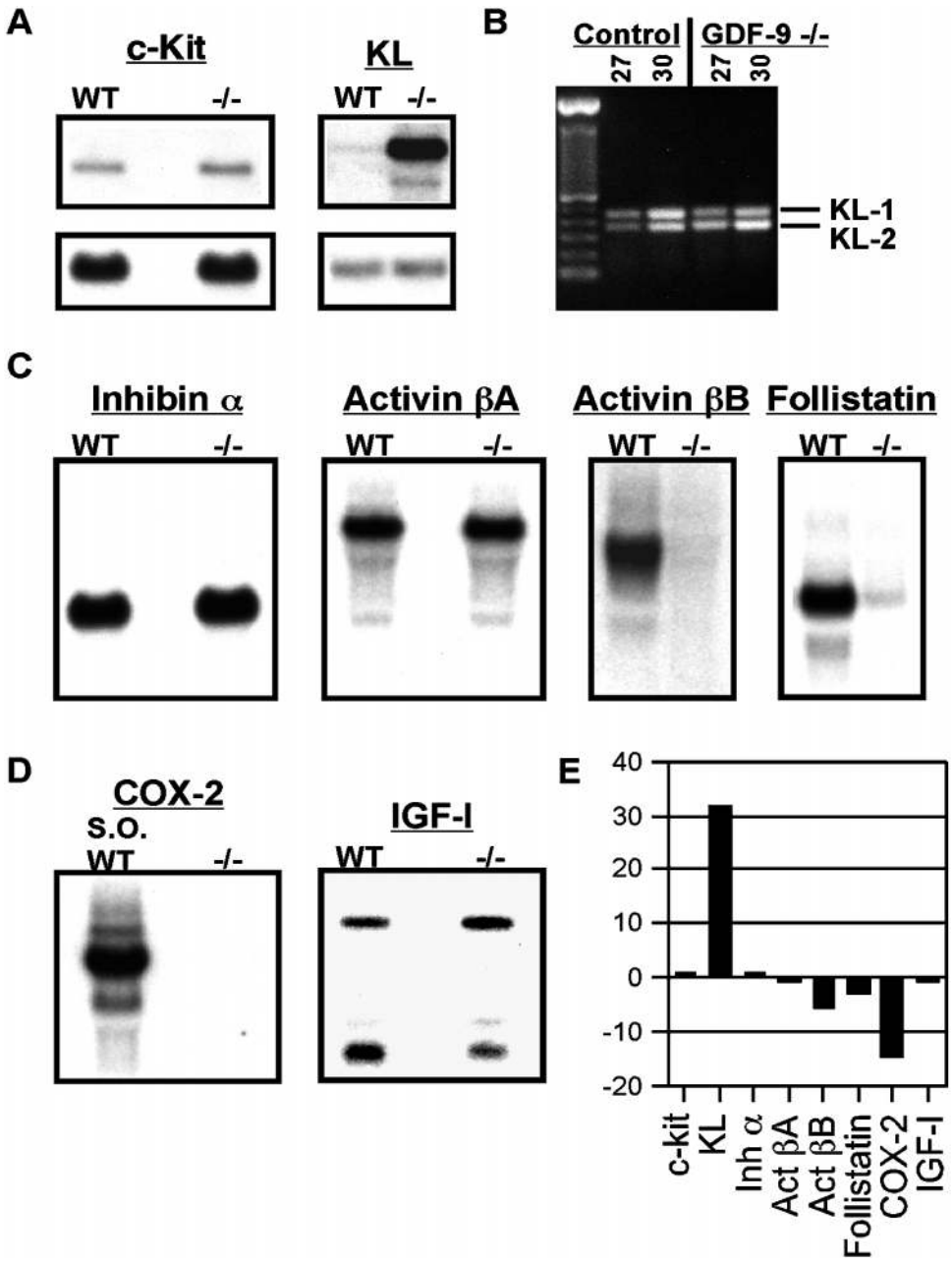

Fig. 3. Analysis of Gene Expression in Control (WT) *vs*. GDF-9-Deficient (−/−) Ovaries

A, Northern blot analysis of c-*kit* and KL gene expression in control and GDF-9-deficient ovaries. The *lower panels* are the GAPDH loading controls. Band intensities (normalized to GAPDH) for GDF-9-deficient: control yields a ratio of 1.4:1 for c-*kit* and 32:1 for KL (E). B, RT-PCR products of control or GDF-9-deficient ovarian RNA amplified for 27 or 30 cycles with primers spanning the alternatively spliced exon, which distinguishes KL-1 from KL-2. Both samples amplify two products of 366 bp and 450 bp, as compared with the 100-bp DNA ladder. C, Northern blot analysis of inhibin α, activin βA, activin βB, and follistatin gene expression in control and GDF-9-deficient ovaries. (GAPDH not shown.) Comparison of band intensities normalized to GAPDH for −/−: control yields a ratio of 1.1:1 for inhibin-α, 1:1.2 for activin-βA, 1:5.9 for activin-βB, and 1:3 for follistatin (E). D, Northern blot analysis of COX-2 in PMSG (48 h)/hCG (5 h)-treated control and GDF-9-deficient ovaries, and IGF-I in unstimulated control and GDF-9-deficient ovaries (18S not shown). The band intensities were normalized to 18S for −/−: control yields a ratio of 1:56 for COX-2 and 1.4:1 for the larger (~7 kb) and 1:1.6 for the lower (~1 kb) forms of IGF-I (E).

quantitative RT-PCR using primers that can distinguish KL-1 from KL-2, we detected both forms of kit ligand in both the wild-type and GDF-9-deficient ovaries (Fig. 3B). Furthermore, immunohistochemical analysis of the KL protein in the GDF-9-deficient ovaries demonstrates the same pattern of expression as the KL mRNA, with the most intense staining occurring in asymmetric follicles (data not shown). Taken to-

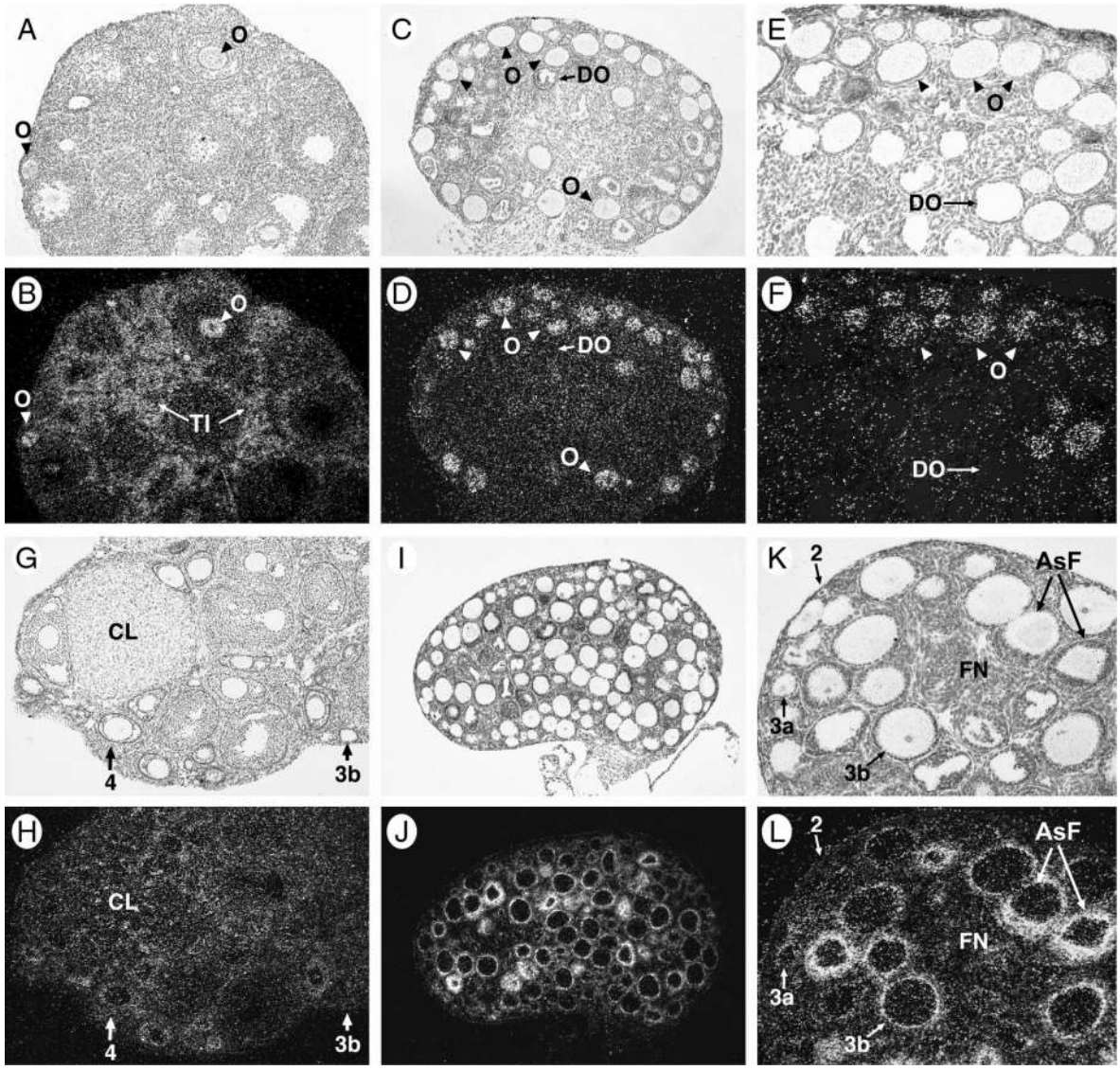

Fig. 4. Localization of c-*kit* and Kit Ligand mRNA

Expression of c-*kit* mRNA in adult control (A and B) and GDF-9-deficient (C–F) ovaries analysis by *in situ* hybridization using specific cDNA antisense probes. (A–D) c-*kit* expression is localized to oocytes (O) in both ovaries, and theca/interstitial cells (TI) in the control (low power). E and F, At higher magnification in the GDF-9-deficient ovary, it is clear that only intact oocytes (O) express c-kit, and that degenerating oocytes (DO) no longer express c-kit (high power). G–L, Expression of kit ligand mRNA in control (G and H) and GDF-9-deficient (I–L) ovaries. G and H, Low levels of KL are expressed in granulosa cells of preantral follicles (*i.e.* type 3b and 4 follicles), scattered cells in the corpus luteum, and in interstitial cells (low power). I–L, In GDF-9-deficient ovaries, the largest type 3b follicles express high levels of KL, and asymmetric follicles (AsF) express even higher levels. The follicular nests (FN) no longer express KL (I and J, low power; K and L, high power).

gether, these results suggest that GDF-9 negatively regulates kit ligand expression in granulosa cells in a paracrine manner and that active, KL protein is synthesized.

TGF-β Superfamily Members (Activins, Inhibins, Follistatin)

Activins and inhibins have been implicated in the regulation of granulosa cell proliferation and follicle growth both *in vivo* and *in vitro* (18, 19). Hence, we compared the expression levels and pattern of expression of inhibin-α, activin-βA, activin-βB, and the activin-binding protein, follistatin, in wild-type and GDF-9-deficient ovaries. Surprisingly, by Northern blot analysis, inhibin-α is expressed at similar levels in GDF-9-deficient *vs.* wild-type ovaries (Fig. 3C). In wild-type ovaries, inhibin α is expressed in granulosa cells of all growing follicles (type 3a through the preovulatory stage), but is excluded from corpora lutea (Fig. 5,

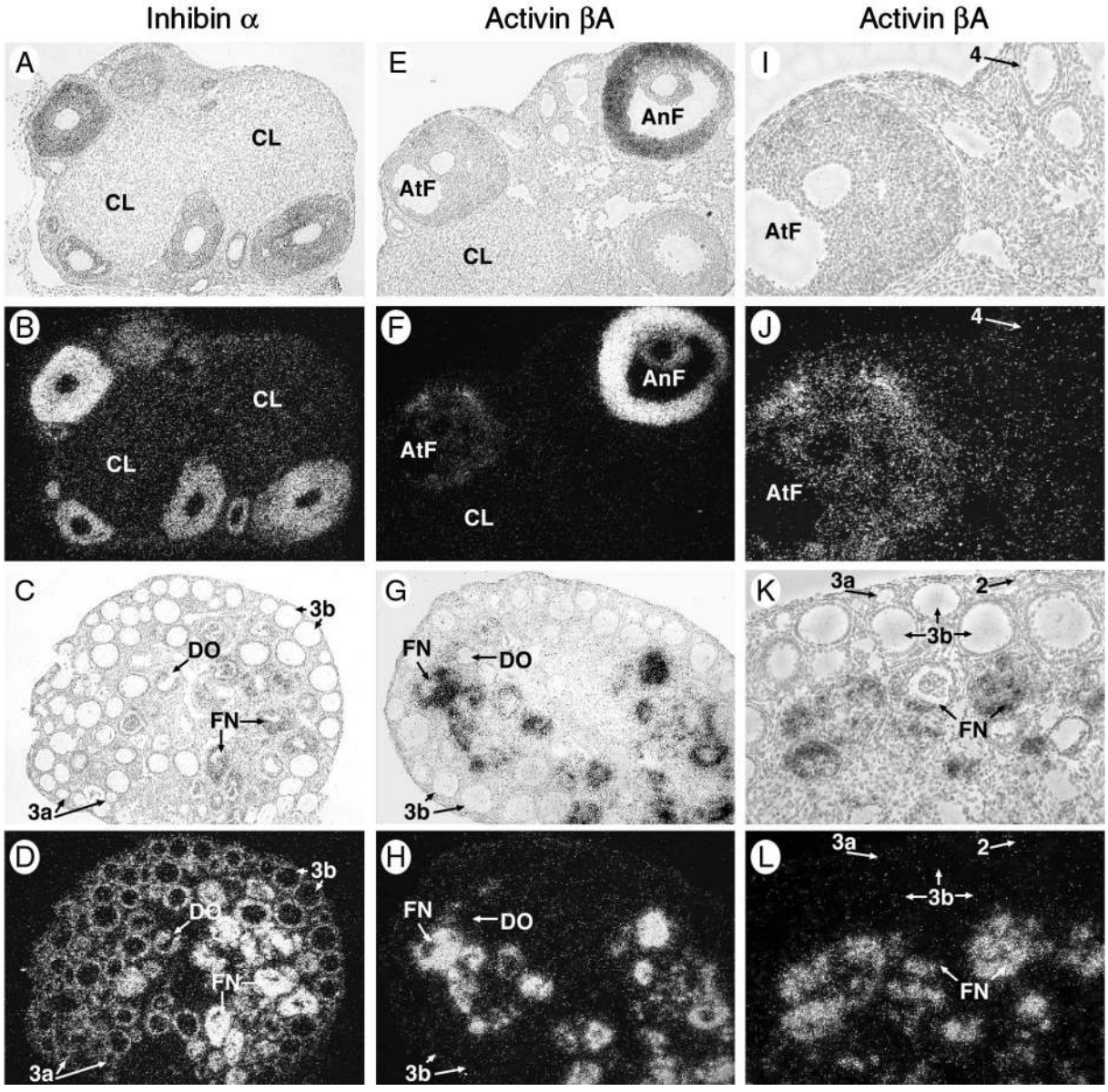

Fig. 5. Localization of Inhibin-α and Activin-βA mRNA

Expression of inhibin-α and activin-βA mRNA in adult control (A, B, E, F, I, and J) and GDF-9-deficient (C, D, G, H, K, and L) ovaries was analyzed by *in situ* hybridization using specific cDNA antisense probes. A and B, Control ovaries show expression of inhibin-α in granulosa cells (GC) of preantral and antral follicles, while cells of the corpora lutea (CL) are negative (low power). C and D, In GDF-9-deficient ovaries, granulosa cells are positive, with follicles with degenerating oocytes (DO) and the follicular nests (FN) having the highest levels of expression (low power). E and F, Expression of activin-βA localizes to granulosa cells of healthy antral follicles (AnF), is less in atretic follicles (AtF), and is absent in corpora lutea of control ovaries (E and F) (low power). At higher magnification (I and J), activin-βA cannot be detected in type 4 follicles. G, H, K, and L, In GDF-9-deficient ovaries, activin-βA is not expressed in primordial (type 2) or one-layer (types 3a and 3b) follicles, but is expressed at low levels in the follicles with degenerating oocytes (DO) and at very high levels in the follicular nests (FN). (G and H, low power; K and L, high power).

A and B). In GDF-9-deficient ovaries, inhibin-α is expressed highly in the one-layer follicles, in the follicles with degenerating oocytes, and in the central steroidogenic follicular nests (Fig. 5, C and D). This indicates that the cells of the follicular nests, although similar to corpora lutea in many respects, are developmentally different than granulosa cells in wild-type ovaries that have proliferated, formed into multilayer follicles, and associated with an active thecal layer before luteinizing.

The two inhibin/activin-β subunits, βA and βB, and the activin binding protein, follistatin, are expressed in overlapping patterns in the wild-type ovary. All three genes are expressed in granulosa cells of multilayer preantral and antral follicles (Fig. 5, E and F, and Fig.

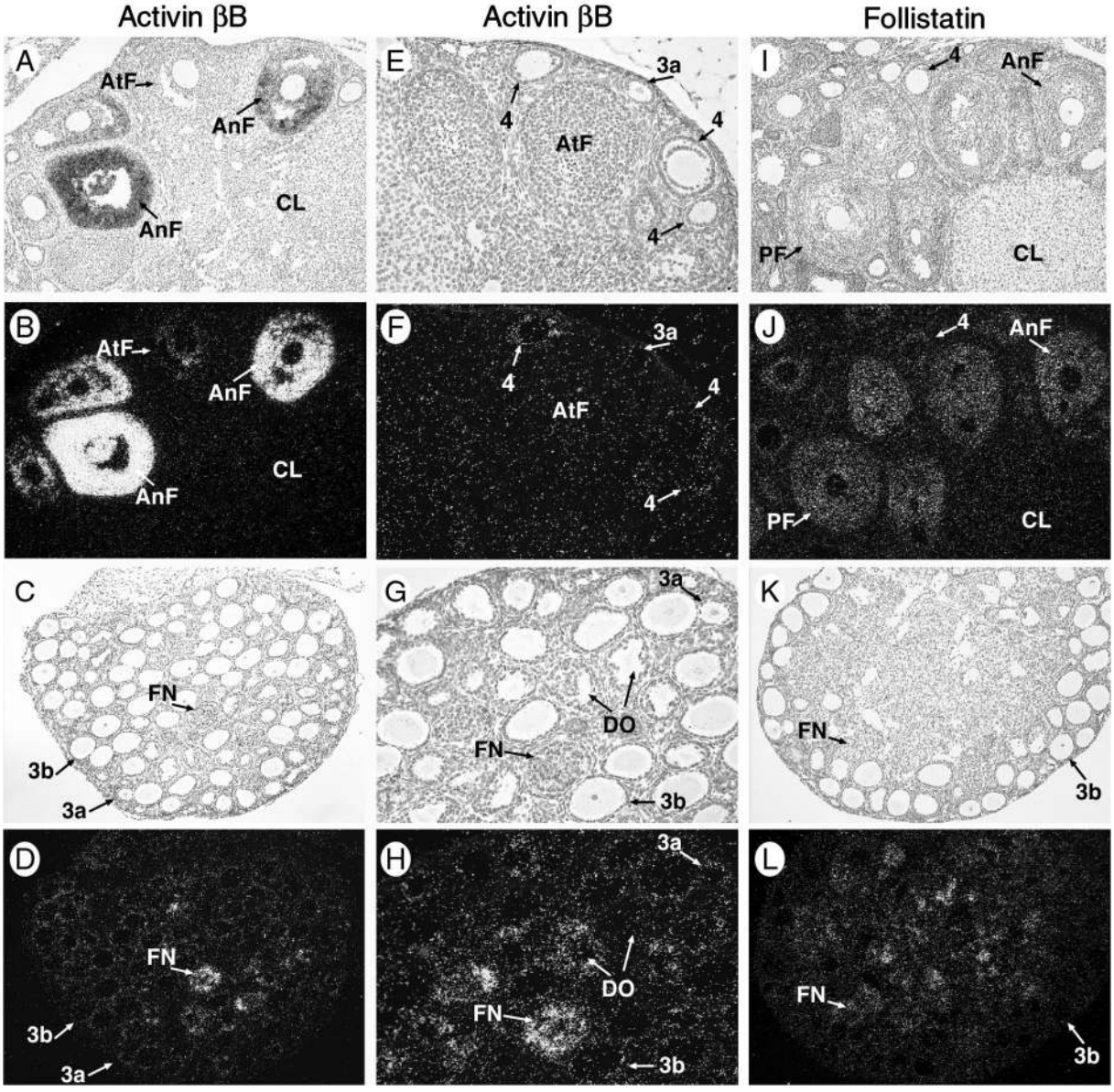

Fig. 6. Localization of Activin-βB and Follistatin mRNA

Expression in adult control (A, B, E, F, I, and J) and GDF-9-deficient (C, D, G, H, K, and L) ovaries was analyzed by *in situ* hybridization using specific cDNA antisense probes. A and B, Control ovaries show high level expression of activin βB in granulosa cells of antral follicles (AnF), while cells of the corpora lutea (CL) and most cells of the atretic follicles (AtF) are negative (low power). E and F, At higher magnification, low levels of activin-βB are detected in two-layer (type 4) follicles. In GDF-9-deficient ovaries, granulosa cells of one- layer (type 3a and 3b) follicles have detectable expression of activin-βB (C and D, low power), while follicles with degenerating oocytes (DO) and follicular nests (FN) have higher levels of expression (G and H, high power). Expression of follistatin localizes to granulosa cells of both preantral follicles (PF) and antral follicles (AnF), but is excluded from the corpus luteum (CL) in control ovaries (I and J). K and L, In GDF-9-deficient ovaries expression localizes to follicles with degenerating oocytes and follicular nests (FN) (low power).

6, A, B, I, and J). Interestingly, expression of βB in atretic follicles is low and localized specifically to the perioocyte cells, while in healthy follicles, all granulosa cells express high levels (Fig. 6, E and F). GDF-9-deficient ovaries have almost undetectable βB-mRNA by Northern blot analysis and very low levels of follistatin (Fig. 3C). These genes are expressed in the granulosa cells of the one-layer follicles, more robustly in follicles with degenerating oocytes, and at highest levels in oocyte-deficient follicular nests (Fig. 6, C, D, G, and H). βA-message is not detectable in the one-layered follicles, weakly localizes to granulosa cells of follicles with degenerating oocytes, and is expressed at high levels in oocyte-deficient follicular nests. However, by Northern blot analysis the levels of βA mRNA are equivalent between GDF-9-deficient and wild-type

ovaries (Fig. 3C). These results indicate that the GDF-9-deficient ovaries have retained the ability to make both activin-β and inhibin-α subunits. However, the relative amounts of each subunit and thus the net production of each type activin (A, B, or AB) or inhibin (A or B) remains to be determined.

Characterization of Antral Follicle Markers (ERβ, FSHR, Cytochrome P-450 Aromatase)

To further characterize the follicles of the GDF-9-deficient ovary, we analyzed the expression of other markers associated with antral granulosa cell functional differentiation: FSH receptor (FSHR), cytochrome P-450 aromatase (aromatase), and estrogen receptor-β (ERβ). We previously showed by Northern blot analysis that FSHR is expressed similarly in both GDF-9-deficient and wild-type ovaries, and that aromatase expression is 50% of the wild-type level (9). ERβ is also expressed at low but similar levels in the knockout *vs.* wild-type ovaries (data not shown). By *in situ* hybridization in the wild-type ovary, we detected FSHR, ERβ, and aromatase specifically in the granulosa cells as previously reported (3, 20, 21). ERβ is expressed at low levels in one-layer follicles and at higher levels in multilayer follicles (Fig. 7, E and F). FSHR is expressed in multilayer preantral and antral follicles (Fig. 7, A and B). Aromatase, which is normally induced by FSH stimulation of the granulosa cells, is expressed at high levels specifically in the preovulatory follicle (Fig. 7, I and J). In the GDF-9-deficient ovary, ERβ is expressed at low levels in the one-layer follicles, and at somewhat higher levels in the follicles with degenerating oocytes (Fig. 7, G and H). FSHR is also expressed in the follicles with degenerating oocytes (Fig. 7, C and D), while aromatase is expressed at high levels only in the follicular nests with completely degenerated oocytes (Fig. 7, K and L). Aromatase expression in these follicular nests in the GDF-9-deficient ovaries suggests that a functional FSH signaling pathway is present similar to granulosa cells of preovulatory follicles of a wild-type ovary.

Characterization of Periovulatory and Luteal Markers [Cyclooxygenase 2 (COX-2), LHR, Cholesterol Side Chain Cleavage Cytochrome P-450]

As mentioned previously, GDF-9-deficient ovaries contain multiple, centrally located nests of cells that have the appearance of luteinized granulosa cells. By electron microscopic analysis, the cells of these nests contain multiple lipid droplets and mitochondria with tubular cristae typical of highly steroidogenic cells (9). To confirm their steroidogenic nature and similarity to luteal cells, we analyzed the expression of COX-2 and LHR message, and cholesterol side chain cleavage cytochrome P-450 protein (P-450 scc). As COX-2 is expressed in the wild-type ovary only within a discrete window of time after the LH surge (22, 23), we used ovaries from 3-week-old mice stimulated for 48 h with PMSG, and then hCG for 5 h for both Northern blot analysis and *in situ* hybridization. By Northern blot analysis, RNA from superovulated ovaries showed three distinct bands, while no bands could be detected in the unstimulated wild-type or GDF-9-deficient ovary lanes (Fig. 3D and data not shown). Consistent with the Northern blot data, *in situ* hybridization shows that in wild-type ovaries stimulated with PMSG and hCG, COX-2 is expressed by the granulosa cells of preovulatory follicles (Fig. 8, A and B and Ref. 23). The highest expression at 5 h occurs in the cumulus cells of the wild-type ovary (Fig. 8, A and B), while COX-2 expression is completely undetectable in the GDF-9-deficient ovary (Fig. 8, C and D).

In contrast to the above-mentioned COX-2 expression data, we have previously shown that LHR is expressed in the GDF-9-deficient ovary at levels comparable to the wild-type ovary by Northern blot analysis (9). LHR is expressed by theca cells, granulosa cells of preovulatory follicles (data not shown), and luteinized granulosa cells of corpora lutea (Fig. 8, E and F) (21). In the GDF-9-deficient ovary, granulosa cells of nonluteinized and luteinized follicular nests express LHR at very high levels (Fig. 8, G and H). Stimulation of theca and luteinized granulosa cells by LH stimulates production of the steroidogenic enzyme P-450 scc and subsequent synthesis of progesterone (3). In wild-type ovaries, P-450 scc protein is present in theca cells, corpora lutea, and secondary interstitial tissue (Fig. 8, I and J). In GDF-9-deficient ovaries, P-450 scc protein is detected at low levels in nonluteinized follicular nests and at much higher levels in the steroidogenic luteinized follicular nests (Fig. 8, K and L). Female 6-week-old GDF-9-deficient mice have average serum progesterone levels of 3.4 ng/ml, compared with 2.6 ng/ml in wild-type mice, indicating that these nests are not only capable of expressing markers but also functioning like miniature corpora lutea. However, as mentioned earlier, these follicular nests also express inhibin-α, a marker that is normally never observed at significant levels in corpora lutea (see below).

DISCUSSION

We have previously demonstrated that absence of GDF-9 in the mammalian oocyte leads to infertility due to a block in follicular development. In the present studies, we attempted to further characterize the defects at the molecular level (summarized in Fig. 9). GDF-9 mRNA (8) and protein (24) are absent in primordial follicles and are first observed in type 3a primary follicles. Ovaries from the GDF-9 knockout mice show a block at the type 3b primary follicle stage. Our studies in this manuscript demonstrate that the granulosa cells of the type 3b follicle essentially lay dormant; neither cell division nor apoptosis is observed in

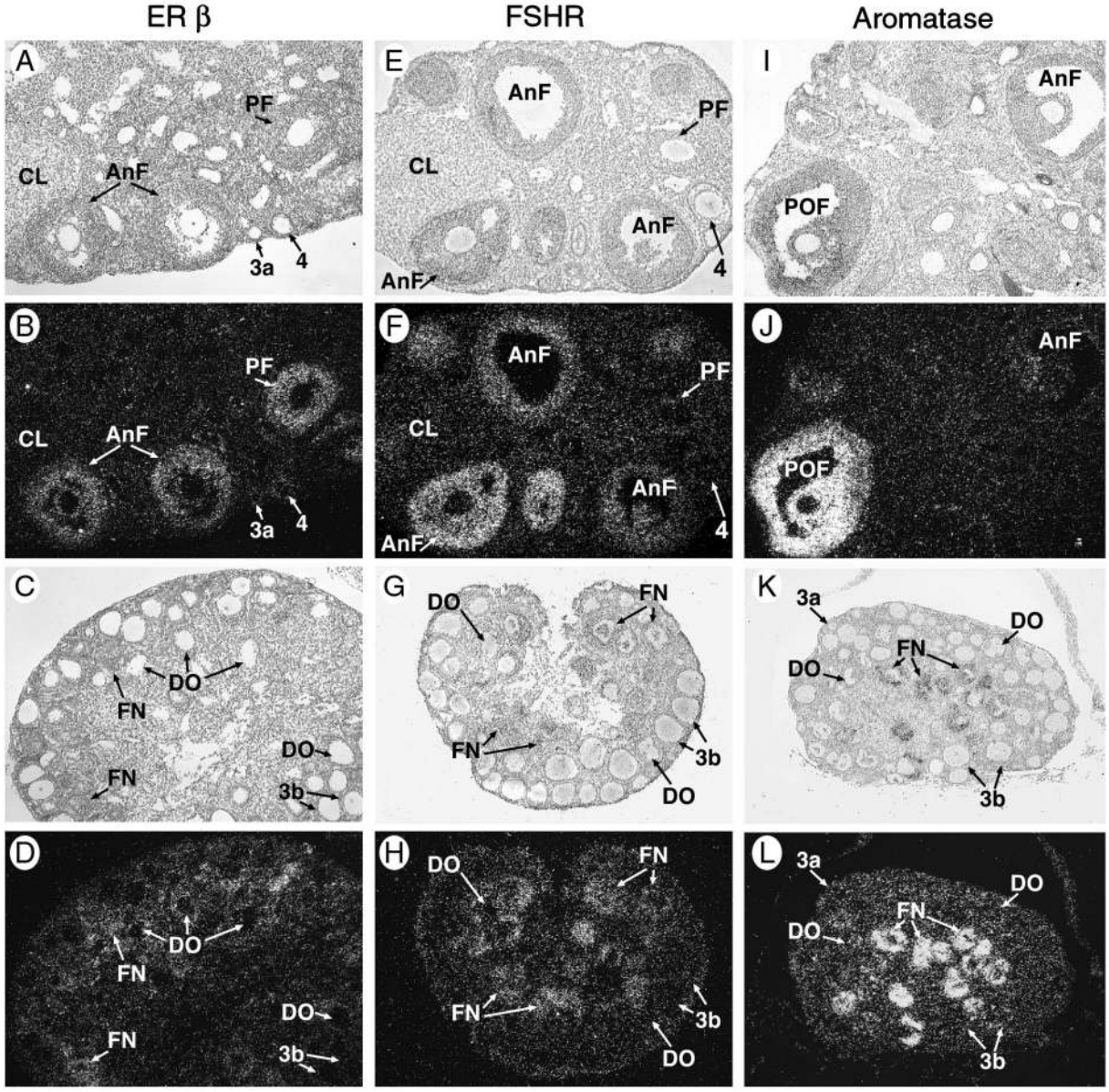

Fig. 7. Localization of Antral Follicle Markers: Estrogen Receptor-β, FSH Receptor, and P-450 Aromatase

Expression in adult control (A, B, E, F, I, and J) and GDF-9-deficient (C, D, G, H, K, and L) ovaries was analyzed by *in situ* hybridization using specific cDNA antisense probes. ERβ expression localizes at low levels to granulosa cells of preantral follicles (PF) including type 3 and type 4 follicles and to antral follicles (AnF) at higher levels (A and B), while FSHR is only detectable in antral follicles (E and F). In GDF-9-deficient ovaries, follicles with degenerating oocytes (DO) and follicular nests (FN) have detectable levels of ERβ (C and D) and FSHR (G and H). I and J, P-450 aromatase is barely detectable in one antral follicle (AnF) of the control ovary, while a larger preovulatory follicle (POF) shows abundant expression. K and L, In the GDF-9-deficient ovary, follicles with degenerating oocytes (DO) show low-level expression of aromatase, but the follicular nests (FN) demonstrate highest expression (low power).

the granulosa cells of the follicles until the oocyte is lost. Thus, although, GDF-9 protein is synthesized at the type 3a stage, the GDF-9 signal transduction cascade must only become essential at the type 3b stage for further follicular growth. Clearly, these studies suggest that recruitment of primordial follicles and growth of the granulosa cells from the primordial follicle stage ($<$20 granulosa cells) to the type 3b stage (90 granulosa cells) (25) are not dependent on GDF-9. Possibly another oocyte-secreted growth factor is required for these approximately two rounds of cell divisions from the primordial to the type 3b primary follicle stage. One factor that may be instrumental in many of these processes is a recently identified transcription factor, FIGα. FIGα mRNA is present in primordial follicles, and FIGα protein has been shown to regulate the transcrip-

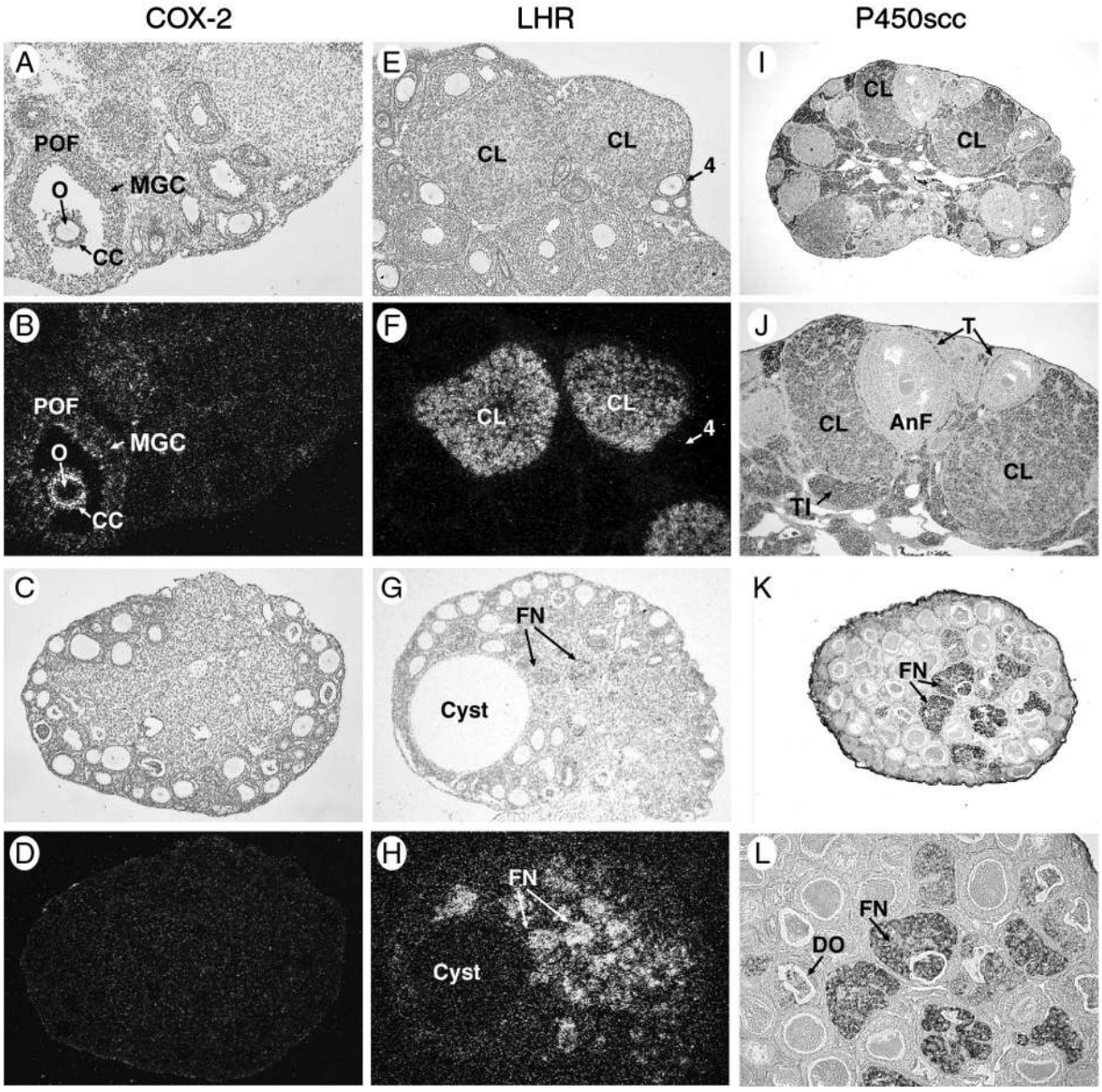

Fig. 8. Localization of Ovulatory and Luteal Markers: COX-2, LHR, and P-450 Cholesterol Side Chain Cleavage

Expression of COX-2 in adult control stimulated with PMSG for 48 h, followed by hCG for 5 h (A, B, E, and F) and unstimulated GDF-9-deficient (C, D, G, and H) ovaries was analyzed by *in situ* hybridization using specific cDNA antisense probes. COX-2 expression localizes to granulosa cells of preovulatory follicles (POF) only, with cumulus cells (CC) surrounding the oocyte (O) expressing higher levels than mural granulosa cells (MGC) (A and B). Sections of GDF-9-deficient ovaries (C and D) failed to demonstrate COX-2 expression and were indistinguishable from sections hybridized with the sense probe (data not shown). E–H, LHR expression is high in corpora lutea (CL) of control ovaries (E and F) and in follicles with degenerating oocytes and in the follicular nests (FN) in the GDF-9-deficient ovaries (G and H) (low power). I–L, P-450 scc protein was detected immunohistochemically (*dark staining*), and sections were not counterstained. In control ovaries, P-450 scc is produced by corpora lutea (CL), theca (T), and interstitial (IC) cells (I, J), but not by preantral or antral granulosa cells. In GDF-9-deficient ovaries, P-450 scc is detectable at low levels in follicles with degenerating oocytes (DO) and at higher levels in the follicular nests (FN) (K and L, low power).

tion of zona pellucida genes. It is likely, in combination with additional factor(s), to regulate the transcription of many other oocyte genes at this stage (26), potentially including a growth factor that signals the pregranulosa cells to initiate replication.

Unlike the dramatic apoptosis observed in atretic follicles of wild-type ovaries, there is minimal apoptosis observed in the GDF-9 knockout ovary. Normally, apoptosis occurs in antral follicles at a point after they become responsive to and dependent on FSH. Even

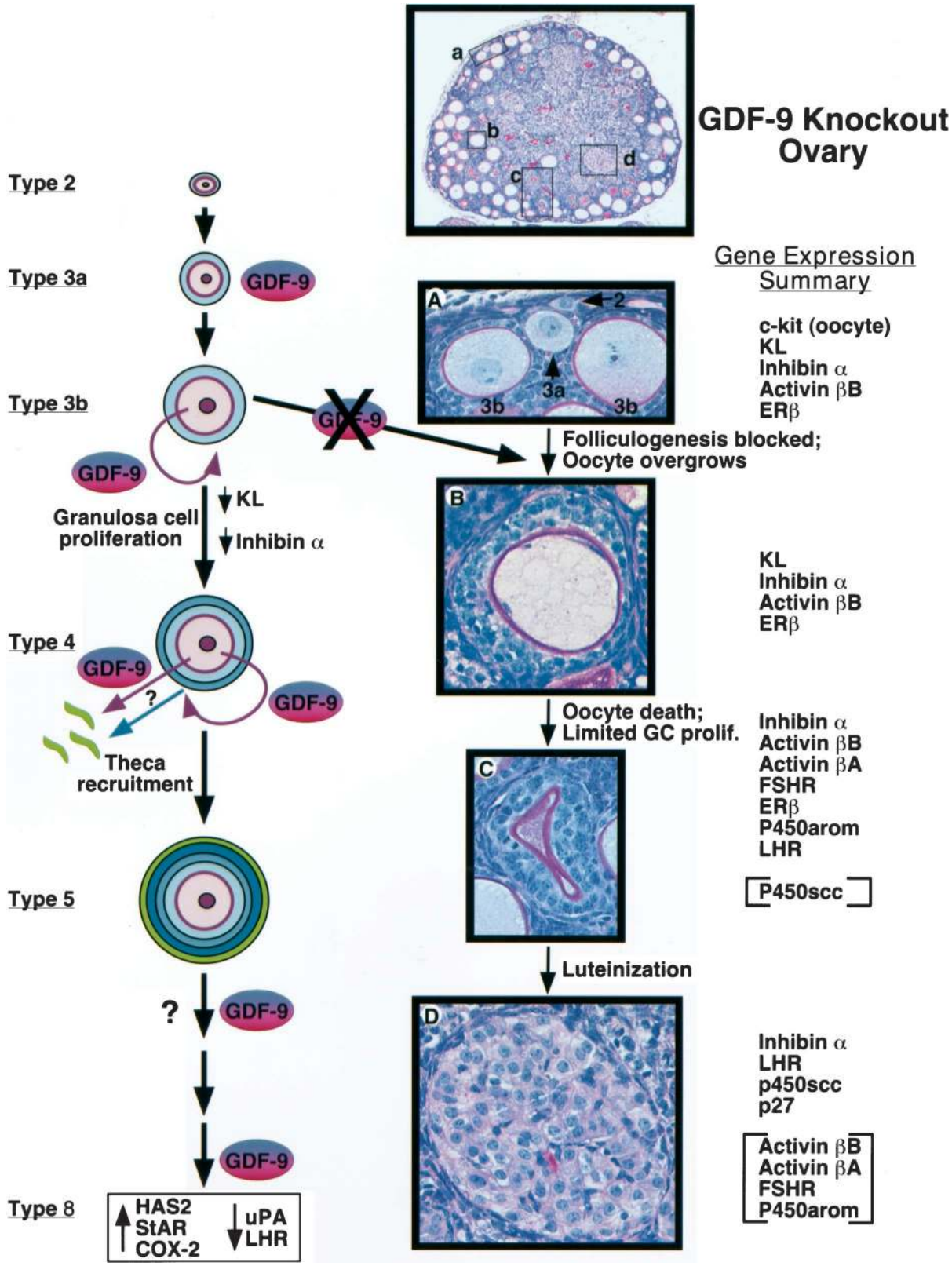

Fig. 9. Summary of the GDF-9 Knockout Ovary Studies

High-power views of the follicles (A and B) and follicular nests (C and D) from PAS-stained sections of GDF-9-deficient ovary. To the *right of each box* is a list of markers expressed at that stage. *Boxes* in low-power image indicate typical location where each follicle type can be found in the GDF-9-deficient ovary (*top*, low power). A, Normal primordial (type 2) and primary follicles (types 3a and 3b). B, A follicle containing an overgrown oocyte with an uneven distribution of granulosa cells. C, A follicular nest

though granulosa cells of the GDF-9-deficient ovary express antral markers, we rarely see apoptotic cells. These observations lead to several alternative explanations. GDF-9 may be required to induce competence to respond to proapoptotic stimuli. Alternatively, although the elevated serum FSH (9) cannot overcome the type 3b block, it may promote granulosa cell survival. Finally, the granulosa cells in the GDF-9-deficient ovaries may bypass this apoptosis-competent state by differentiating after the oocyte degenerates to form the steroidogenic follicular nests. Thus, GDF-9 is an important factor for the differentiation of the granulosa cells, allowing granulosa cells of follicles beyond the type 3b stage to acquire specific characteristics such as the capability to undergo apoptosis.

It has previously been hypothesized that an oocyte-derived factor regulates kit ligand expression by a paracrine mechanism (27). In gonadotropin-stimulated mice, there is a gradient of kit ligand expression whereby granulosa cells farthest from the oocyte (*i.e.* mural granulosa cells) express the highest levels, while those closest to the oocyte (*i.e.* cumulus cells) express very low or undetectable levels (28). Our observations of dramatically elevated kit ligand in GDF-9-deficient follicles suggest that GDF-9 is one of the oocyte-secreted paracrine factors that negatively regulates kit ligand expression. This hypothesis is supported by evidence from our *in vitro* studies of GDF-9 action (see Ref. 24) demonstrating that GDF-9 can regulate other genes (*i.e.* hyaluronan synthase 2, COX-2, steroidogenic acute regulator protein, urokinase plasminogen activator, and LHR) that are differentially expressed with respect to oocyte proximity in antral follicles. Thus, action of other oocyte-produced and extrafollicular factors unopposed by GDF-9 may contribute to the increased kit ligand expression that we observe. The kit ligand that is produced in the GDF-9-deficient ovaries also appears to be active. GDF-9-deficient ovaries contain significantly more mast cells per section (data not shown), possibly due to kit ligand-stimulated increased recruitment and proliferation, as has previously been reported in other systems. In addition, kit ligand has also been shown to stimulate oocyte growth *in vitro* (27). The oocytes in the GDF-9-knockout ovary grow more rapidly and to a 15% greater maximum size compared with the controls (10), before ulitmately degenerating, providing further evidence of functional granulosa cell-derived kit ligand signaling through c-*kit* on the oocyte. By Northern blot analysis, we show that other members of the TGF-β superfamily continue to be expressed in the GDF-9-deficient ovary.

By Northern blot analysis, inhibin-α and activin-βA subunits are expressed in GDF-9-deficient ovaries at similar levels to controls, whereas activin-βB and follistatin are dramatically decreased. *In vitro* activin A has been shown to stimulate follicular growth (18) and to promote FSH stimulation of granulosa cell DNA synthesis (29). Additionally, activin A plus FSH stimulates granulosa cells from immature follicles to produce progesterone, but decreases progesterone synthesis by granulosa cells from differentiated follicles cultured with or without FSH (30). In the GDF-9-deficient ovary, locally produced activin A in the follicular nests may stimulate limited granulosa cell proliferation and enhance the response of these cells to the elevated serum gonadotropins to express P-450 aromatase and P-450 scc. The activin effect in the GDF-9-deficient ovaries may be enhanced by the reduced level of follistatin, an activin-binding protein and antagonist. However, since the follicular nests express both the inhibin-α subunit and activin-βA, it is unclear how much activin A (*vs.* inhibin A) is being produced.

It has been suggested that once a follicle is recruited from the quiescent pool of primordial follicles into the growing pool, there are only two developmental endpoints: cell death or terminal differentiation (1, 25, 31). Follicles normally continue to grow until they either undergo atresia or luteinize after ovulation; under normal circumstances follicles cannot arrest at any intermediate stage. In the GDF-9-deficient ovary, we observe progressive granulosa cell differentiation, albeit uncoupled from granulosa cell proliferation and normal follicular morphogenesis. Evidence suggesting that the oocyte plays a key role in regulating gene expression within the follicle is accumulating. For example, removal of the oocyte from a rabbit follicle *in vivo* triggers luteinization of the follicle (32). In culture, oocytes have also been shown to inhibit expression of LHR (33), a marker of preovulatory follicles and corpora lutea.

There are at least three possible interpretations of our data regarding the functional differentiation of the granulosa cells in the GDF-9-deficient ovary. The first is that the GDF-9-deficient oocytes still produce a factor other than GDF-9 that inhibits granulosa cell differentiation, but when the oocyte degenerates the follicles luteinize. The second possibility is that GDF-9 itself is the luteinization-suppressing agent. The third possibility is that luteinization is one endpoint of a

with an empty zona pellucida remnant (*magenta*) after oocyte degeneration (nonluteinized). D, A luteinized follicular nest containing hypertrophied, foamy-appearing, highly steroidogenic granulosa cells. Model of GDF-9 action in early folliculogenesis (*left*). GDF-9 mRNA and protein are present in type 3a follicles. GDF-9 signaling to the granulosa cells is required for granulosa cell proliferation and growth from the type 3b to type 4 follicle and negatively regulates kit ligand (KL) and inhibin-α expression. Thecal layer recruitment begins at the type 4 follicle stage and may be a direct effect of GDF-9 (*purple arrow*) or alternatively GDF-9 may induce the granulosa cells to produce a recruitment factor (*blue arrow*). The role of GDF-9 in larger preantral and antral follicles is still unknown. In the preovulatory follicle (type 8), GDF-9 stimulates hyaluronan synthase 2 (HAS2), steroidogenic acute regulatory protein (StAR), and COX-2 and suppresses LHR and urokinase plasminogen activator (uPA) (24).

default pathway that every granulosa cell follows in a cell-autonomous manner after awakening from quiescence, and that regulation of the process occurs by inducing cell death before the granulosa cells reach that endpoint. Whatever the reason for luteinization, the progression to a luteinized phenotype is not simply turning on the genes that we see in the fully differentiated corpus luteum, but a progressive process in which markers of intermediate stages of follicles are expressed. For example, serial sections (data not shown) hybridized with probes for aromatase, LHR, and P-45017αOH, showed distinct aromatase-positive, LHR-negative; aromatase-positive, LHR-positive; and aromatase-negative, LHR-positive follicular nests (all were 17αOH negative). Additionally, aromatase and FSHR, both markers of antral follicles, appear preferentially expressed in degenerating oocyte-containing or nonluteinized follicular nests (Fig. 9, ovary panel C) rather than the more steroidogenic-appearing, fully luteinized nests (Fig. 9, ovary panel D). In the wild-type ovary, the morphology of the follicle (*i.e.* number of granulosa cell layers, antrum, presence or absence of an oocyte) has allowed us to classify granulosa cell markers. However, in the GDF-9-deficient ovary, follicular nests that are at different stages of differentiation may histologically look very similar. For this reason, it may appear that both luteinized and nonluteinized markers are being abnormally coexpressed, especially for markers such as aromatase and FSHR in which there is some variability in the prevalence of expressing clusters. However, the widespread expression of inhibin-α, a marker clearly excluded from the CL in the wild-type ovary in the majority of the central clusters, suggests that the luteal clusters are not identical to normal CL. This suggests that some luteal cell markers are actively suppressed, and this inhibitory factor is not present or the cells are not responsive to it.

In the GDF-9-knockout, the thecal layer fails to form as determined by light and electron microscopy and absence of the thecal layer markers P-450 17α-hydroxylase, LHR, and c-*kit* around the one-layer type 3b follicles. However, 17α-hydroxylase-positive cells, presumed theca cell precursors, are still present throughout the interstitium. These data suggest that GDF-9, either directly or indirectly, regulates thecal layer development (Fig. 9). Previous studies have suggested that a preantral follicle-derived factor is necessary for thecal layer formation and that follicles with more than two layers of granulosa cells, but not one-layer follicles, appear to be more competent at stimulating thecal layer formation (34). Thus, absence of a thecal layer could be due to the failure of GDF-9 to stimulate the formation of a type 4 follicle and/or the secretion of the theca cell recruitment factor. Based on its expression in granulosa cells of preantral follicles, kit ligand is a candidate thecal layer recruitment factor. However, our findings that kit ligand is highly expressed in the GDF-9-knockout ovary makes this possibility unlikely. The finding that theca precursor cells are still present suggests that intragonadal and extragonadal factors continue to normally regulate differentiation and gene expression (*i.e.* 17α-hydroxylase expression) in these cells.The present studies open up new avenues of research for understanding ovarian function and the intraovarian role of GDF-9. Future studies will include determining the factors that are required for the regulation of primordial follicle recruitment and the development of the thecal layer during ovarian folliculogenesis and the interactions of GDF-9 in these processes.

MATERIALS AND METHODS

Experimental Animals

All experimental mice were maintained in accordance with the NIH Guide for the Care and Use of Laboratory Animals. Unless otherwise indicated, ovaries from adult C57Bl/6/129SvEv hybrid mice 6–12 weeks of age were used for both RNA isolation and specimens for *in situ* hybridization and immunohistochemistry. For the studies of COX-2, 3-week-old mice received ip injections of 7.5 IU Gestyl (Diosynth B.V., Oss, Holland), and then with 5 IU of hCG (Sigma Chemical Co., St. Louis, MO) 48 h later. Ovaries were collected 5 h after hCG injection.

RNA Isolation and Northern Blot Analysis

Total RNA was extracted from various tissues of wild-type and GDF-9–deficient C57BL/6/129SvEv hybrid mice using RNA STAT-60 (Leedo Medical Laboratories, Houston, TX) as described by the manufacturer and quantitated on a spectrophotometer. Fifteen micrograms of total RNA of each sample were electrophoresed on a 1.2% agarose/7.6% formaldehyde gel and transferred to Hybond N nylon membrane (Amersham, Arlington Heights, IL). Table 1 includes a summary of all the specific cDNA fragments used to make probes in these studies. Probes were generated by random priming with [α^{32}P]dATP using the Strip-EZ probe synthesis kit (Ambion, Inc., Austin, TX). The membrane was hybridized, washed, and subjected to autoradiography as previously described (35). The probe was removed from the membrane using the Strip-EZ removal reagents (Ambion, Inc.) following the manufacturer's protocol. The same blots were then reprobed with glyceraldehyde-3-phosphate dehydrogenase (GAPDH) or 18S ribosomal RNA as a loading control. Signals for each probe were quantitated on a Molecular Dynamics, Inc. (Sunnyvale, CA) photodensitometer.

In Situ Hybridization

In situ hybridization was performed essentially as described previously (36) with the following modifications. Freshly dissected ovaries from wild-type or GDF-9-deficient C57Bl/6/129SvEv hybrid mice were fixed in 4% paraformaldehyde-PBS overnight, processed, and embedded in paraffin. Sections (5 μm thick) were cut and pretreated as described. Table 1 includes a summary of the specific probe information. [α-^{35}S]UTP-labeled antisense and sense probes were generated using the Riboprobe T7/T3 or Riboprobe T7/SP6 Combination System (Promega Corp., Madison, WI). Hybridization was carried out at 55 C with 5×10^6 cpm of each riboprobe per slide for 16–18 h in 50% deionized formamide/0.3 M NaCl/20 mM Tris-HCl (pH 8.0)/5 mM EDTA/10 mM $NaPO_4$ (pH 8.0)/10% Dextran sulfate/1$\times$ Denhardt's/0.5 mg/ml yeast

Table 1. Northern Blot and *in Situ* Probes

Probe	Length (bp)	Source	Reference
p27	594	Dr. W. Harper	1–594 of U09968
P-450 17α-OH	522	Dr. A. Payne (subcloned)	0–522 of M64863
c-*kit*	462	PCR	1050–1512 of Y00864
Kit ligand	476	PCR	78–554 of M57647
Inhibin α	630	Subcloned from gene	931–1043 of M95526
Activin βA	425	Subcloned from cDNA	1049–1474 of X69619
Activin βB	836	PCR	1–602 of X83376 + 240 bp upstream
Follistatin	1032	PCR	1–1032 of Z29532
ERβ	347	Dr. S.K. Dey	164–511 of AJ000220
FSHR	800	PCR	367-1266 of AF095642
P-450 Aromatase	618	PCR	42–660 of D00659
COX-2	864	Dr. S.K. Dey	65–929 of M94967
LHR	750	PCR	592–1331 of M81310
IGF-I	376	Drs. J. Zhou and C. Bondy	(37)

All probes used in this manuscript are murine.

RNA. High-stringency washes of 2× SSC/50% formamide and 0.1× SSC at 65 C were carried out. Dehydrated sections were dipped in NTB-2 autoradiographic emulsion (Eastman Kodak Co., Rochester, NY) and exposed 2–14 days, depending on the probe, at 4 C. After developing, the slides were counterstained with hematoxylin and mounted for photography.

Immunohistochemistry

Ovaries were fixed in 20% neutral buffered formalin for 3 h, processed, embedded in paraffin, and sectioned at 4 μm thickness. Detection of PCNA was conducted as previously described (38) using a mouse anti-PCNA monoclonal antibody (Novocastra Laboratories, Newcastle upon Tyne, UK). The rabbit antimouse P-450 scc polyclonal antiserum was a kind gift from Michael J. Soares at the University of Kansas Medical Center, and used at a 1:625 dilution in 1× PBS, 0.05% Tween-20 (PBST), with 2% normal mouse serum (Sigma Chemical Co.) and 2% normal goat serum (Vector Laboratories, Inc., Burlingame, GA). Rabbit anti-Ki-67 polyclonal antiserum (Novocastra) was diluted 1:300 and rabbit anti-p27 polyclonal antiserum (Santa Cruz Biotechnology, Inc., Santa Cruz, CA) was diluted 1:125 in 1% BSA, 0.1% NaN_3 in PBS, with 2% normal mouse serum and 2% normal goat serum. Successful staining for both Ki-67 and p27 required antigen retrieval methods. For Ki-67 staining, sections were steamed for 35 min in 0.1 M citrate buffer, pH 6.0. For p27 staining, sections were steamed for 35 min in pH 8.0 Tris-EDTA antigen retrieval solution. For Ki-67, p27, and P-450 scc, all sections were blocked for 30 min in 1× PBS with 0.05% Tween-20, 2% normal mouse serum (Sigma Chemical Co.), and 2% normal goat serum and incubated with the primary antibody for 1 h at room temperature. PCNA detection was accomplished using the Super Sensitive Mouse Antibody Animal Detection kit (BioGenex Laboratories, Inc., San Ramon, CA) containing antimouse IgG-biotinylated secondary antibody preabsorbed with rat tissue. P-450 scc, p27, and Ki-67 antibodies were detected using the Super Sensitive Rabbit Antibody Detection kit (Biogenex Laboratories, Inc.) containing antirabbit IgG-biotinylated secondary antibody preabsorbed with mouse tissue. PCNA and P-450 scc were detected using streptavidin-conjugated alkaline phosphatase label and New Fuschin substrate (BioGenex Laboratories, Inc.) while p27 was detected with streptavidin-conjugated horseradish peroxidase label (BioGenex Laboratories, Inc.) and 3,3′-diaminobenzidine tetrahydrochloride substrate (Vector Laboratories, Inc.).

TUNEL Assay

Ovaries were stained for apoptotic cells by a modified TUNEL method using the Apoptag Plus Complete Apoptosis Detection kit (Oncor Laboratories, Gaithersburg, MD) following the manufacturer's instructions. Nuclei were counterstained with Propidium iodide/Antifade mounting media (Oncor Laboratories).

RT-PCR Analysis

Oligo-dT-primed cDNA from 1 μg of either control or GDF-9-deficient ovarian RNA was synthesized using Superscript reverse transcriptase (Gibco BRL, Gaithersburg, MD) following the manufacturer's protocol. One microliter of each RT reaction (1/20 of total) was used in each 25 μl PCR reaction primed with kit ligand-specific oligonucleotides: 5′-CCAGAAACTAGATCCTTTACTCCT-3′(sense, nucleotides 493–517 of S40364) and 5′-CTGTTGCAGCCAGCTCCCT-TAG-3′ (antisense, nucleotides 943–919 of S40364) primers which span introns and an 84-bp alternatively spliced exon. Amplification of the KL-1 form yields a product of 450 bp, and amplification of KL-2 form yields a product of 366 bp. Products were separated on a 2% agarose gel and visualized by ethidium bromide staining.

Acknowledgments

We thank Drs. Carolyn Bondy, S. K. Dey, Wade Harper, Anita Payne, and Jian Zhou for the gifts of the cDNA probes; Dr. Michael Soares for the anti-P-450 scc antibody; Rebecca Robker and Dr. Joanne Richards for teaching us the *in situ* hybridization technique; Kim Paes for help with figures; Shirley Baker for aid in manuscript preparation; and Drs. T. Rajendra Kumar and Joanne Richards for critical review of the manuscript.

Received February 1, 1999. Revision received March 22, 1999. Accepted March 24, 1999.

Address requests for reprints to: Martin M. Matzuk, M.D., Ph.D., Professor, Department of Pathology, Baylor College of Medicine, One Baylor Plaza, Houston, TX 77030. E-mail: mmatzuk@bcm.tmc.edu.

These studies were supported in part by sponsored research grants from Genetics Institute (Cambridge, MA) and Metamorphix (Baltimore, MD) and NIH Grant HD-33438 (to

M.M.M.). Julia A. Elvin is a student in the Medical Scientist Training Program supported in part by NIH Grants GM-07330 and GM-08307 and the Baylor Research Advocates for Student Scientists (BRASS) organization.

REFERENCES

1. Hirshfield AN 1991 Development of follicles in the mammalian ovary. Int Rev Cytol 124:43–101
2. Adashi EY 1992 Intraovarian peptides. Stimulators and inhibitors of follicular growth and differentiation. Endocrinol Metab Clin North Am 21:1–17
3. Richards JS 1994 Hormonal control of gene expression in the ovary. Endocr Rev 15:725–751
4. Dube JL, Wang P, Elvin J, Lyons KM, Celeste AJ, Matzuk MM 1998 The bone morphogenetic protein 15 is X-linked and expressed in oocytes. Mol Endocrinol 12:1809–1817
5. Lau AL, Shou W, Guo Q, Matzuk MM 1997 Transgenic approaches to study the functions of the transforming growth factor β superfamily members. In: Aono T, Sugino H, and Vale WW (eds) Inhibin, Activin, and Follistatin: Regulatory Functions in System and Cell Biology. Springer-Verlag, Inc., New York, pp 220–243
6. Elvin JA, Matzuk MM 1998 Mouse models of ovarian failure. Rev Reprod 3:183–195
7. Lyons KM, Pelton RW, Hogan BLM 1989 Patterns of expression of murine Vgr-1 and BMP-2a RNA suggest that transforming growth factor-β-like genes coordinately regulate aspects of embryonic development. Genes Dev 3:1657–1668
8. McGrath SA, Esquela AF, Lee S-J 1995 Oocyte-specific expression of growth/differentiation factor-9. Mol Endocrinol 9:131–136
9. Dong J, Albertini DF, Nishimori K, Kumar TR, Lu N, Matzuk MM 1996 Growth differentiation factor-9 is required during early ovarian folliculogenesis. Nature 383:531–535
10. Carabatsos M, Elvin J, Matzuk M, Albertini D 1998 Characterization of oocyte and follicle development in growth differentiation factor-9-deficient mice. Dev Biol 203:373–384
11. Oktay K, Schenken RS, Nelson JF 1995 Proliferating cell nuclear antigen marks the initiation of follicular growth in the rat. Biol Reprod 53:295–301
12. Gerdes J, Lemke H, Baisch H, Wacker HH, Schwab U, Stein H 1984 Cell cycle analysis of a cell proliferation-associated human nuclear antigen defined by the monoclonal antibody Ki-67. J Immunol 133:1710–1715
13. Robker RL, Richards JS 1998 Hormonal control of the cell cycle in ovarian cells: proliferation versus differentiation. Biol Reprod 59:476–482
14. Besmer P, Manova K, Duttlinger R, Huang EJ, Packer A, Gyssler C, Bachvarova RF 1993 The *kit*-ligand (steel-factor) and its receptor c-*kit*/*W*: pleiotropic roles in gametogenesis and melanogenesis. Devel Suppl:125–137
15. Huang EJ, Manova K, Packer AI, Sanchez S, Bachvarova RF, Besmer P 1993 The murine steel panda mutation affects kit ligand expression and growth of early ovarian follicles. Dev Biol 157:100–109
16. Kuroda H, Terada N, Nakayama H, Matsumoto K, Kitamura Y 1988 Infertility due to growth arrest of ovarian follicles in the *Sl*/*Sl*^{t} mice. Dev Biol 126:71–79
17. Manova K, Nocka K, Besmer P, Bachvarova RF 1990 Gonadal expression of c-*kit* encoded at the *W* locus of the mouse. Development 110:1057–1069
18. Mather JP, Moore A, Li RH 1997 Activins, inhibins, and follistatins: further thoughts on a growing family of regulators. Proc Soc Exp Biol Med 215:209–222
19. Matzuk MM, Kumar TR, Shou W, Coerver KA, Lau AL, Behringer RR, Finegold MJ 1996 Transgenic models to study the roles of inhibins and activins in reproduction, oncogenesis, and development. Recent Prog Horm Res 51:123–157
20. Byers M, Kuiper G, Gustafsson J-A, Park-Sarge O-K 1997 Estrogen receptor-β mRNA expression in rat ovary: down-regulated by gonadotropins. Mol Endocrinol 11:172–182
21. Camp T, Rahal J, Mayo K 1991 Cellular localization and hormonal regulation of follicle-stimulating hormone and luteinizing hormone receptor messenger RNAs in the rat ovary. Mol Endocrinol 5:1405–1417
22. Sirois J, Simmons DL, Richards JS 1992 Hormonal regulation of messenger ribonucleic acid encoding a novel isoform of prostaglandin endoperoxide H synthase in rat preovulatory follicles. J Biol Chem 267:11586–11592
23. Sterneck E, Tessarollo L, Johnson PF 1997 An essential role for C/EBPβ in female reproduction. Genes Dev 11:2153–2162
24. Elvin JA, Clark AT, Wang P, Wolfman N, Matzuk MM 1999 Paracrine actions of growth differentiation factor-9 in the mammalian ovary. Mol Endocrinol 13:1035–1048
25. Pedersen T 1972 Follicle growth in the mouse ovary. In: Biggers JD, Shuetz AW (eds) Oogenesis. University Park Press, Baltimore, pp 361–376
26. Liang L, Soyal S, Dean J 1997 FIGα, a germ cell specific transcription factor involved in the coordinate expression of the zona pellucida genes. Development 124:4939–4947
27. Packer AI, Hsu YC, Besmer P, Bachvarova RF 1994 The ligand of the c-*kit* receptor promotes oocyte growth. Dev Biol 161:194–205
28. Motro B, Bernstein A 1993 Dynamic changes in ovarian c-*kit* and *steel* expression during the estrous reproductive cycle. Dev Dynam 197:69–79
29. Miro F, Hillier S 1996 Modulation of granulosa cell deoxyribonucleic acid synthesis and differentiation by activin. Endocrinology 137:464–468
30. Miro F, Smyth C, Hillier S 1991 Development-related effects of recombinant activin on steroid synthesis in rat granulosa cells. Endocrinology 129:3388–3394
31. Peters H, Byskov AG Himelstein-Braw R Faber M 1975 Follicular growth: the basic event in the mouse and human ovary. J Reprod Fertil 45:559–566
32. El-Fouly MA, Cook B, Nekola M, Nalbandov AV 1970 Role of the ovum in follicular luteinization. Endocrinology 87:288–293
33. Eppig JJ, Pendola FL, Wigglesworth K 1998 Mouse oocytes suppress cAMP-induced expression of LH receptor mRNA by granulosa cells *in vitro*. Mol Reprod Dev 49:327–332
34. Magarelli PC, Zachow RJ, Magoffin DA 1996 Developmental and hormonal regulation of rat theca-cell differentiation factor secretion in ovarian follicles. Biol Reprod 55:416–420
35. Mahmoudi M, Lin VK 1989 Comparison of two different hybridization systems in northern transfer analysis. Biotechniques 7:331–332
36. Albrecht U, Eichele G, Helms JA, Lu HC 1997 Visualization of gene expression patterns by *in situ* hybridization. In: Daston GP (ed) Molecular and Cellular Methods in Developmental Toxicology. CRC Press, Boca Raton, FL, pp. 23–48
37. Zhou J, Chin E, Bondy CA 1991 Cellular pattern of IGF-I and IGF-I receptor gene expression in the developing and mature follicle. Endocrinology 129:3281–3288
38. Robker RL, Richards JS 1998 Hormone-induced proliferation and differentiation of granulosa cells: a coordinated balance of the cell cycle regulators cyclin D2 and p27^{KIP1}. Mol Endocrinol 12:924–940